Aalborg Universitet

Reliable Control of Ship-mounted Satellite Tracking Antenna

Soltani, Mohsen; Izadi-Zamanabadi, Roozbeh; Wisniewski, Rafal

Reliable Control of Ship-Mounted Satellite Tracking Antenna

Mohsen N. Soltani, *Member, IEEE*, Roozbeh Izadi-Zamanabadi, and Rafael Wisniewski

Abstract—Motorized antenna is a key element in overseas satellite telecommunication. The control system directs the on-board antenna toward a chosen satellite while the high sea waves disturb the antenna. Certain faults (communication system malfunction or signal blocking) cause interruption in the communication connection resulting in loss of the tracking functionality, and instability of the antenna. In this brief, a fault tolerant control (FTC) system is proposed for the satellite tracking antenna. The FTC system maintains the tracking functionality by employing proper control strategy. A robust fault diagnosis system is designed to supervise the FTC system. The employed fault diagnosis solution is able to estimate the faults for a class of nonlinear systems acting under external disturbances. Effectiveness of the method is verified through implementation and test on an antenna system.

Index Terms—Antenna, fault tolerant control (FTC), nonlinear internal model, robust fault diagnosis, tracking.

I. INTRODUCTION

THE ABILITY to maintain communication over large distances has always been an important issue. Tracking of the satellite is a *must* for sustaining contact with it. In marine communication, movements of a ship, partly generated by waves, will force the antenna to point away from the satellite and thereby break the communication. The problem is addressed by developing a dedicated control algorithm that uses the received signals from the satellite.

Another problem arises when the signal is blocked due to change in atmosphere, or a physical hurdle between the antenna and satellite. This results in feeding the faulty data to the control loop and hence leading to the loss of tracking functionality and instability. An fault tolerant control (FTC) system, which is a combination of fault diagnosis and accommodation units, is proposed in this article. This system detects the fault and reconfigures the control system in order to maintain antenna direction toward the satellite during the fault period.

A nonlinear internal model control (NIMC) is suggested to be used for the faulty case scenario. NIMC is able to handle uncertainties in the plant parameters [1, Sec. 1.1]. We address the design of an NIMC similar to that of [2], where a model-based design is considered. NIMC is capable of rejecting the dominant disturbances which are ship's roll, pitch, and yaw motions detected in the base of the antenna (see [3] and [4]).

A particular focus of this brief is on designing an FDI system (see, e.g., [5] and [6]) for the satellite tracking antenna (STA)

that not only is able to handle the nonlinearity but also is robust to the uncertainties and disturbances. An application of nonlinear fault tolerant control design based on internal model control theory is presented in [7]. The control reconfiguration in [7] is achieved by designing a controller which is implicitly tolerant against the faults whose model is embedded in the regulator. In our work, we employ a classical concept to FDI and FTC which is based on the explicit estimation of unknown time varying parameters and explicit reconfiguration of the controller. A geometric approach for fault diagnosis in nonlinear systems is developed in [8]–[11]. Unknown input observers are developed in [10]–[12] to estimate the fault. These methods succeed to estimate/detect the faults for those cases where the frequency information of the fault does not have to be taken into account. In this brief, the fault diagnosis is applied on the STA system to detect parametric faults using the frequency information of the fault. The proposed $\mathcal{H}_\infty$ optimization method in [13] and [14] for the nonlinear system's fault detection has been employed. To the best of our knowledge, no application of this approach to any physical nonlinear system has been reported. In addition, the problem of distinguishing faults from disturbances has been addressed in this article. This is an original contribution to the mentioned nonlinear FDI approach. To illustrate the potential of the presented method, the FTC system is verified against a real antenna system with success.

This brief is organized as follows. In Section II, the problem statement is presented. The dynamical model of the operating STA, the beam control strategy, and the fault nature is addressed in Section III. Section IV devices the proposed FDI method and the FDI design procedure. In Section V, the FTC scenario along with NIMC design are described. Section VI presents the results in practical tests and analyzes the FDI design. Concluding remarks are provided in the last section of this brief.

II. PROBLEM STATEMENT

Given a communication antenna platform, develop a fault-tolerant control system that reliably detects a class of commonly occurred faults and accommodates them by means of control reconfiguration.

The solution to the stated problem is achieved by addressing the following three specific objectives:

- development of a comprehensive model that adequately describes the dynamic/kinematic behavior of the antenna system;
- development of fault diagnosis algorithms that detect the faults while being robust toward system uncertainties and external disturbances;
- development of an alternative control strategy for the nonlinear system suitable for reconfiguration purposes.
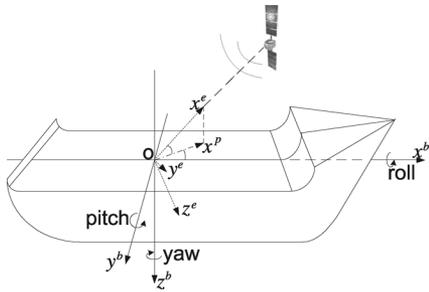
Fig. 1. Body-fixed frame F^b and Earth frame F^e.

A. Notation

Let I be the identity matrix of a required dimension. We designate the vector space of n by n matrices with real entries by $M(n, \mathbb{R})$, and the special orthogonal group by $SO(3) = \{R \in M(3, \mathbb{R}) : RR^T = I, \det(R) = 1\}$. The rotation matrices describing rotation from a coordinate system a to a coordinate system b will be denoted by $R_{ab} \in SO(3)$. Since R_{ab} is an orthogonal matrix $R_{ba} = R_{ab}^{-1} = R_{ab}^T$. The diagonal matrix with entries $a_1, \dots, a_n$ on the diagonal is denoted by $\mathrm{diag}(a_1, \dots, a_n)$.

III. SATELLITE TRACKING ANTENNA (STA) SYSTEM

The prerequisite for designing the model-based fault diagnosis and control algorithm is a comprehensive model for the system's behavior. In the first part of this section the model for the STA is derived. Verification results in [15] showed that the proposed dynamic model closely simulates the real system. In the second part we briefly describe the conventional control strategy for the STA system. In addition, the effect of faults is discussed.

A. Modeling of STA

To describe the relationship between satellite position, antenna element direction and ship disturbances, a common fixed inertial coordinate system is needed. Earth frame F^e describes the position of the satellite in an Earth-fixed frame with the origin in the base of the antenna. Since, the chosen satellite is geostationary, its position is fixed in F^e. We use the fact that the translative movements of the origin of F^e (ship) is negligible compared with the distance between ship and satellite. Furthermore, x^e is pointing toward the satellite and y^e and z^e are vectors orthogonal to x^e where ye lays on the horizontal plane as shown in Fig. 1. Body-fixed frame F^b describes the orientation of the hull to the earth fixed frame. The origin of this frame is placed in the base of the antenna. The vector x^b is the heading vector of the ship, y^b is the right side vector of the ship, and z^b is pointing downward the ship. Fig. 1 shows the frame F^b with respect to the ship. The axes y^e and z^e can be made aligned with y^b and z^b by two rotations of F^e around y^b and z^b axes. The rotation between frames F^b and F^e is caused by the waves and wind affecting the dynamics of the ship motion. This rotation is described by the rotation matrix R_{eb} by

$$\dot{R}_{eb} = R_{eb}\mathrm{Skew}(\omega_{eb}^b) \tag{1}$$

where ω_{eb}^b is the angular velocity vector of F^b relative to F^e, resolved in F^b, [16, Sec. 16.4]

$$\omega_{eb}^b = \begin{bmatrix} p & q & r \end{bmatrix}^T$$

where p, q, and r are roll, pitch, and yaw angular velocities respectively, illustrated in Fig. 1. The map Skew is defined by

$$\mathrm{Skew}(\omega_{eb}^b) = \begin{bmatrix} 0 & -r & q \\ r & 0 & -p \\ -q & p & 0 \end{bmatrix}.$$
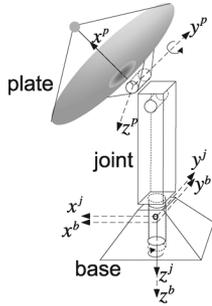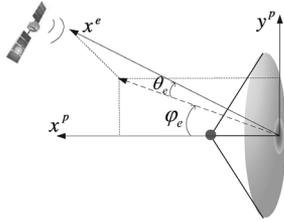
When analyzing the ship motions at sea, at least three contributions to the movement should be considered: The wind acting on the ship, the waves generated by the wind, and the currents at sea. In several works these contributions have been modeled by stochastic processes [17, Sec. 4.2]. However, the resulting motion of the ship itself, caused by the wind, waves, and the current, is far less documented for generic purposes. The reason is that differences in ship structures, sizes and loads affect the dynamic behavior of the ships significantly. The main contributor to the ship motion is the wave acting on the hull. To simplify the model, it is assumed that the waves are the only disturbances acting on the ship, but at the same time it is ensured that the disturbance specifications, provided by Inmarsat [18], are met. The roll and pitch disturbances affecting the dynamics of the ship are known to be locally well modeled by two sinusoidal waves (see also [3], [4], and [17, Sec. 4.2]). One of the sinusoidal waves has a short periodic length of about 6 s and the other is in the range of 8 to 10 s. Likewise, the yaw disturbance can be modeled as a single sinusoidal wave. Briefly, the waves acting on the ship can be modeled by

$$\dot{w} = Sw \tag{2}$$

where $w = \begin{bmatrix} p & \dot{p} & q & \dot{q} & r & \dot{r} \end{bmatrix}^T$, $S = \mathrm{diag}(S_i)$, $i = 1, 2, 3$, and

$$S_i = \begin{bmatrix} 0 & \Omega_i \\ -\Omega_i & 0 \end{bmatrix} \tag{3}$$

where Ω_1, Ω_2, and Ω_3 are the frequencies of roll, pitch, and yaw disturbances. The initial value of w determines the phase of sinusoids. This system will be called the *exosystem*. In conclusion, disturbances generate rotation between F^e and F^b given by (1) and (2), where ω_{eb}^b and w are related by $\omega_{eb}^b = \begin{bmatrix} p & q & r \end{bmatrix}^T$. To describe the orientation of the antenna element direction, two frames are defined: *Joint* frame F^j and *Plate* frame F^p. The origin of F^j is placed in the antenna joint geometrical center and the vector z^j is aligned with z^b. The frame F^j rotates with respect to F^b around z^b axis by the azimuth motor as shown in Fig. 2. The angle of rotation θ_{bj}^j can be measured directly from the motor. The rotation is expressed by the rotation matrix R_{bj}, [16, p. 412]. The origin of F^p is placed in the center of the antenna plate. The vector y^p is aligned with the vector y^j. The axis x^p is perpendicular to the plate of the antenna [which is also called the antenna line of sight (LOS)]. The frame F^p rotates with respect to F^j around y^p axis by the elevation motor. The angle of rotation θ_{jp}^p can be measured directly from the motor.

This article has been accepted for inclusion in a future issue of this journal. Content is final as presented, with the exception of pagination.

SOLTANI *et al.*: RELIABLE CONTROL OF SHIP-MOUNTED SATELLITE TRACKING ANTENNA 3

Fig. 2. Joint frame F^j and Plate frame F^p.

Fig. 3. Illustration of error angles θ_e and ϕ_e.

The rotation is expressed by the rotation matrix R_{jp}, [16, p. 413].

The dynamics of the motors and kinematics of the antenna have been analyzed in [15]. Due to the inherent characteristics of the employed motors, here step-motors, their dynamics are simplified as $\dot{\theta}_{bj}^j = u_{bj}^j$ and $\dot{\theta}_{jp}^p = u_{jp}^p$, where u_{bj}^j and u_{jp}^p are the inputs of the azimuth and elevation motors, respectively.

In order to define the control problem of the ship-mounted STA, the tracking error is subsequently formulated. The beam sensor measures the error angles between x^e and the antenna line of sight x^p. The sensor outputs are two angles ϕ_e and θ_e. ϕ_e is the angle between x^p and the projection of x^e on the plane XY^p spanned by x^p and y^p. θ_e is the angle between x^e and its projection on XY^p, as shown in Fig. 3. Clearly, we can calculate the unit vector x^e in F^p by

$$(x^e)^p = v^p = \begin{bmatrix} \cos(\phi_e)\cos(\theta_e) \\ \sin(\phi_e)\cos(\theta_e) \\ \sin(\theta_e) \end{bmatrix}.$$

Thus, error angles are $\phi_e = \tan^{-1}([0 \ 1 \ 0]v^p / [1 \ 0 \ 0]v^p)$ and $\theta_e = \sin^{-1}([0 \ 0 \ 1]v^p)$.

On the other hand, we can calculate v^p from the vector x^e in F^e by $v^p = R_{pe}(x^e)^e = R_{pe}[1 \ 0 \ 0]^T$, where R_{pe} is the rotation matrix from F^e to F^p characterized by joints and ship orientation. It is given by $R_{pe} = R_{pj}R_{jb}R_{be}$. The nonlinear dynamics of the STA system is defined as follows:

$$\dot{x} = \mathbf{f}(x, u, w) \qquad e = \mathbf{h}(x) \qquad y = \mathbf{k}(x) \qquad \dot{w} = Sw \quad (4)$$

where $x = (x^1, x^2) \in \mathbb{R}^2 \times SO(3)$ with $x^1 = (\theta_{bj}^j, \ \theta_{jp}^p)$ and $x^2 = R_{be}$, $u = (u_{bj}^j, u_{jp}^p) \in \mathbb{R}^2$ is the input vector to the motors, $w \in \mathbb{R}^6$ is the vector of exogenous system states, $e = (\phi_e, \theta_e) \in \mathbb{R}^2$ is the vector of the output error from the beam sensor, and $y = (\theta_{bj}^j, \theta_{jp}^p, \phi_e, \theta_e) \in \mathbb{R}^4$ is the measurement
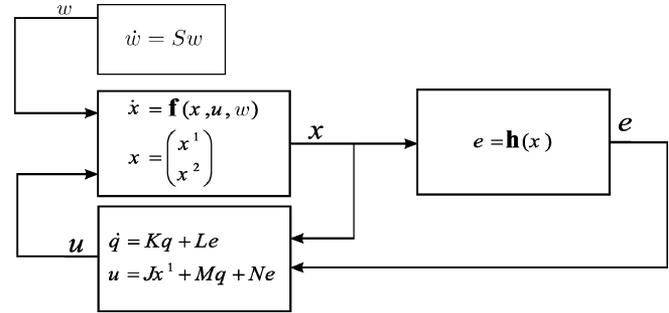

Fig. 4. Block diagram of the antenna model.

vector. Furthermore, the nonlinear smooth functions $\mathbf{f}, \mathbf{h}$, and $\mathbf{k}$ are expressed as follows:

$$\mathbf{f} : \mathbb{R}^2 \times SO(3) \times \mathbb{R}^3 \to \mathbb{R}^2 \times SO(3), \quad \mathbf{f}(x, u, \omega_{eb}^b)$$
$$= (\mathbf{f}^1(u), \mathbf{f}^2(x^2, \omega_{eb}^b)) = (u, -\text{Skew}(\omega_{eb}^b)x^2) \quad (5)$$
$$\mathbf{h} : \mathbb{R}^2 \times SO(3) \to \mathbb{R}^2, \quad \mathbf{h}(x)$$
$$= \begin{bmatrix} \tan^{-1}\left(\frac{-x_{11}^2 \sin(x_1^1)\cos(x_2^1) + x_{21}^2 \cos(x_1^1)\cos(x_2^1)}{x_{11}^2 \cos(x_1^1)\cos(x_2^1) + x_{21}^2 \sin(x_1^1)\cos(x_2^1) + x_{31}^2 \sin(x_2^1)} \right) \\ \sin^{-1}\left(\frac{-x_{11}^2 \cos(x_1^1)\sin(x_2^1) - x_{21}^2 \sin(x_1^1)\sin(x_2^1) + x_{31}^2 \cos(x_2^1)}{1} \right) \end{bmatrix}$$
$$(6)$$

and

$$\mathbf{k} : \mathbb{R}^2 \times SO(3) \to \mathbb{R}^4, \quad \mathbf{k}(x) = (x^1, h(x)). \quad (7)$$

B. Beam Control

In the normal operation scenario, the controller utilizes the measurement of the output error from the beam sensor to regulate the antenna direction toward the satellite (see Fig. 4). The control system is designed for the linearized model of the antenna about an equilibrium point. To simplify the model, the rotation matrix R_{be} is considered as the disturbance input. The linearized model of the STA system around the equilibrium point $x^{1*} = 0, x^{2*} = I$, and $u^* = 0$ is

$$\dot{x}^1 = u \qquad e = \bar{C}x^1 + \Sigma_{i=1}^3 \bar{D}_i x_i^2 \qquad y = \begin{bmatrix} x^1 \\ e \end{bmatrix} \quad (8)$$

where $\bar{C} = d\mathbf{h}/dx^1|_{x^*}$, $\bar{D}_i = d\mathbf{h}/dx_i^2|_{x^*}$, and x_i^2 is the ith column of x^2. The original control problem was solved by designing a robust feedback controller of the form

$$\dot{q} = Kq + Le \qquad u = Jx^1 + Mq + Ne \quad (9)$$

so that the error e vanishes to zero as $t \to \infty$. The matrices J, K, L, M, and N are obtained by solving the standard $\mathcal{H}_\infty$ control problem for the linear system (8). The first equation of (8) is an integrator thus it is not necessary to include x^1 in the first equation of (9) to obtain asymptotic tracking of the step input.

C. Fault Discussion

A failure in the beam sensor means that the pointing error feedback from the satellite is unknown and, hence, can lead to the loss of high bandwidth communication link depending.
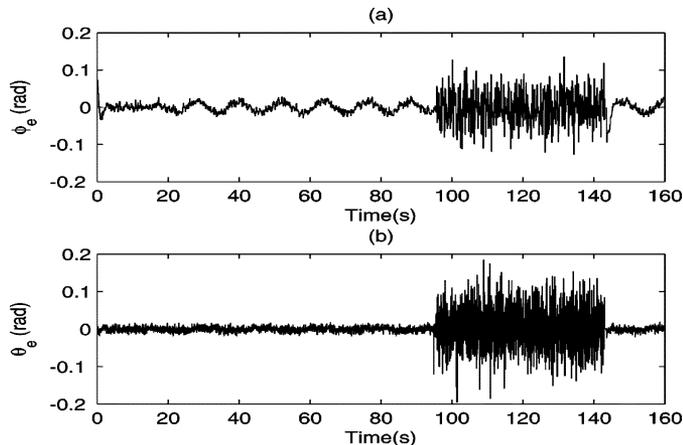
This article has been accepted for inclusion in a future issue of this journal. Content is final as presented, with the exception of pagination.

4   IEEE TRANSACTIONS ON CONTROL SYSTEMS TECHNOLOGY

Fig. 5.   Faulty beam sensor measurement: (a) elevation error ϕ_e and (b) cross-elevation error θ_e.

Fig. 6.   Spectrum of the faulty/non-faulty beam sensor signal: (a) elevation error ϕ_e and (b) cross-elevation error θ_e.

In order to maintain a good strength of the satellite signal that reaches the antenna, the controller keeps the pointing error between the antenna and the satellite below one degree. A change in the strength of the signal measured by the beam sensor can occur by means of the so-called signal blocking. Signal blocking can occur due to: 1) appearance of any hurdle between the antenna and the satellite and 2) changes in the atmospheric pressure and temperature. Blocking results in an increase of the fluctuations in the pointing error measurement due to loss of signal strength. However, this increase depends on the strength of the signal reaching the antenna plate during blocking. In general, deviations due to disturbances and initial conditions from the satellite sight vector cause the same fluctuations. But they should not be considered as blocking since the controller will compensate for those deviations. This is the main reason for not utilizing detection methods that only use the statistical properties of the measurement signals for detecting the mentioned blocking faults. The effect of signal blocking faults on the beam sensor output are shown in Fig. 5(a) and (b), where the fault is injected to the STA system as interruption in signal transmission in the time interval 96 to 144 s. A spectral analysis of the beam sensor signal in both faulty and non-faulty cases is shown in Fig. 6. These analyses show that the fault effects the measurements at higher frequencies.

To establish a model for fault, we analyze the frequency band in which the fault has clearly an impact. We observe that the magnitude of high frequency noise increases. We assign an uncertainty parameter to represent the normalized variance of the error signal. The normalized variance is obtained by dividing the variance of the error signal by its variance in the worst case of fault scenario. Experimental study shows that the worst case fault scenario is when the communicating satellite is shut down. It is obtained empirically by emulating the faulty scenario on the antenna system.

Thus, the parameters which have to be estimated are $-1 \leq \delta_{f_1} \leq 1$ and $-1 \leq \delta_{f_2} \leq 1$, where $|\delta_{f_1}|^2$ $(|\delta_{f_2}|^2)$ is the variance of the elevation (cross-elevation) error signals when the fault occurs.
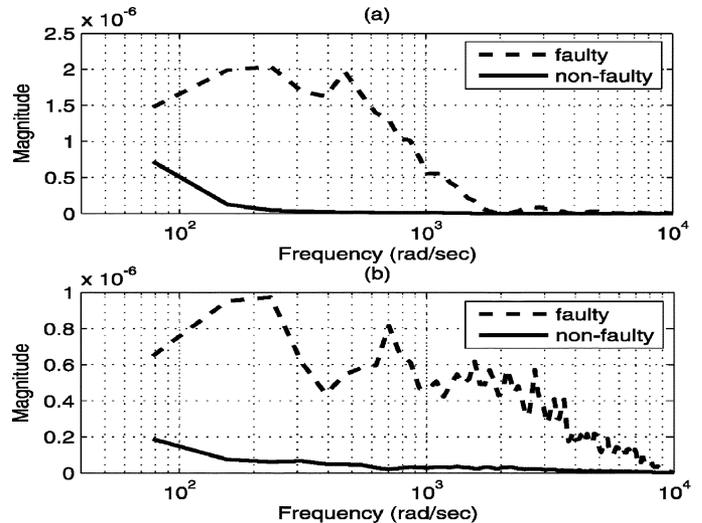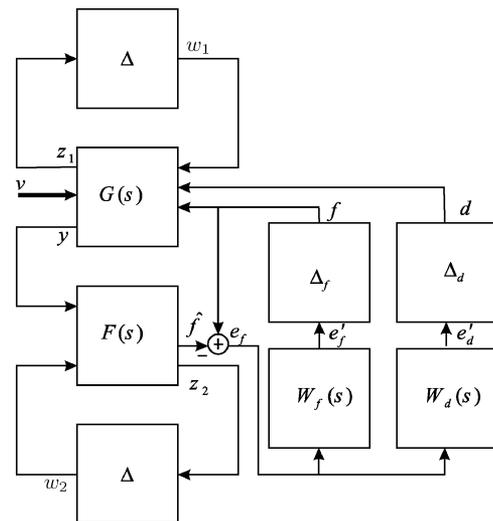

Fig. 7.   Block diagram of the FDI system in robust standard setup.

IV. ROBUST FAULT DIAGNOSIS

A. Standard Setup Formulation

The generalized concept of fault detection architecture in a class of nonlinear systems (proposed in [13]) is employed in this section. In this setup (see Fig. 7), the upper block Δ represents the nonlinearity that is assumed to be sector bounded in an $\mathcal{H}_\infty$ sense [19, Sec. 5.3]. The assumption in this method, (see [14]), is that the stability of the nonlinear system is inferred from robust stability of the linear model $G(s)$ in an LFT with respect to Δ.

The block $F(s)$ in Fig. 7 is the FDI filter to be designed which will be combined with a copy of the nonlinear block Δ. The signal $\hat{f}$ is the estimation of f (fault effect on the error signal) which is generated by FDI system. Defining e_f as $e_f = f - \hat{f}$, the design objective is now to make e_f sufficiently small for any bounded f. The signal d is the disturbance affecting the

This article has been accepted for inclusion in a future issue of this journal. Content is final as presented, with the exception of pagination.

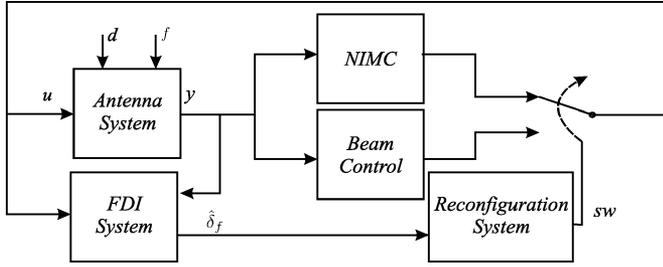SOLTANI *et al.*: RELIABLE CONTROL OF SHIP-MOUNTED SATELLITE TRACKING ANTENNA

5

Fig. 8.   STA system reconfiguration overview.

error signal. The blocks W_f and W_d are the weighting functions that, based on the design criteria, are used to distinguish between fault and disturbance. These two blocks are in fact the gains of the filtered error estimations. The filter W_f (W_d) amplifies in the frequency band of the fault (disturbance). These filters can be obtained from the fault and disturbance spectra of the test facility. We augment the system with Δ_f and Δ_d which are the fictitious fault and disturbance uncertainty blocks, respectively, and assuming that $\|\Delta_f\|_\infty \le 1$ and $\|\Delta_d\|_\infty \le 1$ are norm bounded. Now, it is possible to find a linear filter which solves a μ problem for a linear system structure including four uncertainty blocks, i.e., two Δ blocks combined with Δ_f and Δ_d in Fig. 7. In fact, it is possible to write the system as

$$\begin{bmatrix} \tilde{z} \\ \tilde{y} \end{bmatrix} = \tilde{G}(s) \begin{bmatrix} \tilde{w} \\ \tilde{u} \end{bmatrix} \tag{10}$$

where $\tilde{z} = [z_1\ z_2\ é_f\ é_d]^T$, $\tilde{y} = [y\ w_2]^T$, $\tilde{w} = [v\ w_1\ w_2\ f\ d]^T$, and $\tilde{u} = [\hat{f}\ z_2]^T$. The design of the FDI filter follows the result in [14].

Theorem 1: Assume that the system

$$\tilde{G}(s) = \begin{bmatrix} \tilde{G}_{\tilde{z}\tilde{w}}(s) & \tilde{G}_{\tilde{z}\tilde{u}}(s) \\ \tilde{G}_{\tilde{y}\tilde{w}}(s) & \tilde{G}_{\tilde{y}\tilde{u}}(s) \end{bmatrix} \tag{11}$$

and the linear filter $F(s)$ satisfy

$$\left\| \tilde{G}_{\tilde{z}\tilde{w}}(s) + \tilde{G}_{\tilde{z}\tilde{u}}(s)F(s)\tilde{G}_{\tilde{y}\tilde{w}}(s) \right\|_\mu < \gamma$$

then the $\mathcal{L}_2 - \mathcal{L}_2$ operator gain from fault f to fault estimation error e_f when applying the FDI system in Fig. 7 is bounded also by γ.

B. Design of FDI Filter for the STA System

The first step of the design procedure is to separate the linear and nonlinear parts of the system. This complies with the assumption that the nonlinear part is sector bounded. Considering the system dynamics, there are two nonlinear parts in $\mathbf{f}^2(\cdot)$ and $\mathbf{h}(\cdot)$. The outputs provided by these two functions are always norm-bounded ($x^2 \in SO(3)$ and $\mathbf{h}(x)$ is a composition of $\tan^{-1}$ and $\sin^{-1}$). Thus, the nonlinear sector of the system is bounded. Using (8) and (9), we write the linear part as

$$\dot{x}^1 = Jx^1 + Mq + Ne \qquad \dot{q} = Kq + Le. \tag{12}$$

The output error e is modeled as

$$e = \mathbf{h}(x) + f + d \tag{13}$$

where f is the fault and d is the disturbance on the output error. To separate the nonlinear part of e in the Δ block, we first introduce a fictitious input v (assumed to be bounded), then write (13) as

$$e = w_1 + f + d \tag{14}$$

where $w_1 = \mathbf{h}(x)z_1$ and $z_1 = v$. (For simplicity, the artificial input signal v is injected as a unit step input. In general, the boundedness of w_1 has to be satisfied. Note that $\mathbf{h}(x)$ is the nonlinearity which is represented by Δ so $w_1 = \Delta z_1$). Combining (12) and (13), the dynamics can be written as

$$\dot{x}^1 = Jx^1 + Mq + N\Delta z_1 + N\Delta_f é_f + N\Delta_d é_d$$
$$\dot{q} = Kq + L\Delta z_1 + L\Delta_f é_f + L\Delta_d é_d. \tag{15}$$

The second step is to write the whole system in a standard setup so that it can be used by the linear robust design tools such as μ synthesis [20]. This setup is formulated as (for more detail the reader is referred to [21])

$$\begin{bmatrix} \dot{\tilde{x}} \\ \tilde{z} \\ \tilde{y} \end{bmatrix} = \begin{bmatrix} A & B_1 & B_2 \\ C_1 & D_{11} & D_{12} \\ C_2 & D_{21} & D_{22} \end{bmatrix} \begin{bmatrix} \tilde{x} \\ \tilde{w} \\ \tilde{u} \end{bmatrix} \tag{16}$$

where $\tilde{x} = [x^1\ q\ x_{ef}\ x_{ed}]^T$ (that x_{ef} and x_{ed} are the states of W_f and W_d filters, respectively) and $\tilde{w} = \hat{\tilde{\Delta}}\tilde{z}$ with $\hat{\tilde{\Delta}} = \text{diag}(\Delta, \Delta, \Delta_f, \Delta_d)$.

The last step is to compute the fault detection filter by D-K algorithm. Hence, the solution is to apply standard D-K iterations by assuming $\Delta = \text{diag}(\delta_i)$, $\Delta_f = \text{diag}(\delta_{f_i})$, and $\Delta_d = \text{diag}(\delta_{d_i})$, where all δ_i, δ_{f_i}, and δ_{d_i} belong to unit circle in the complex plane for $i = 1, 2$.

V. CONTROL RECONFIGURATION

When signal blocking fault occurs, the beam control system (9) becomes unstable as it uses the faulty beam sensor data. The accommodation strategy for the FTC system is to switch to another control system in order to maintain the satellite direction. A NIMC controller, which does not use the beam sensor data, is developed in this section. The overview of the reconfigurable system is shown in Fig. 8, where the reconfiguration system uses a threshold on the estimated fault variance $\hat{\delta}_f$ to decide whether the system is faulty.

A. Nonlinear Internal Model Control

Consider the system (4) and suppose that there exists a controller of the form

$$\dot{\xi} = \varphi(\xi, y) \qquad u = \vartheta(\xi, y) \tag{17}$$

in which $\varphi(\cdot, \cdot)$ and $\vartheta(\cdot, \cdot)$ are smooth functions, satisfying $\varphi(0,0) = 0$ and $\vartheta(0,0) = 0$. Then, the generalized tracking problem is as follows.

Given the system (4) with exosystem (2), and two sets $\mathcal{X} \subset \mathbb{R}^n$ and $\mathcal{W} \subset \mathbb{R}^r$, find a controller of the form (17) and a subset $\mathcal{E} \subset \mathbb{R}^v$, such that, in the closed-loop:
1) the trajectory $(x(t), \xi(t), w(t))$ is bounded;
2) $\lim_{t \to \infty} e(t) = 0$;

This article has been accepted for inclusion in a future issue of this journal. Content is final as presented, with the exception of pagination.

6   IEEE TRANSACTIONS ON CONTROL SYSTEMS TECHNOLOGY

for every initial condition $(x(0), \xi(0), w(0)) \in \mathcal{X} \times \mathcal{E} \times \mathcal{W}$ (see [1, Sec. 1.3]). The solution to the generalized tracking problem is given by NIMC. Let $\pi : \mathbb{R}^r \to \mathbb{R}^n$ and $\sigma : \mathbb{R}^r \to \mathbb{R}^v$ be two smooth maps, and suppose that the smooth manifold $\mathcal{M}_0 = \{(x, \xi, w) : x = \pi(w), \xi = \sigma(w)\}$ is invariant for the forced closed-loop system (4) with (17). $\mathcal{M}_0$ is invariant for the closed-loop system means that $\pi(w)$ and $\sigma(w)$ are solutions of the pair of differential equations

$$\frac{\partial \pi}{\partial w} Sw = \mathbf{f}(\pi(w), \vartheta(\sigma(w), \mathbf{k}(\pi(w))), w)$$
$$\frac{\partial \sigma}{\partial w} Sw = \varphi(\sigma(w), \mathbf{k}(\pi(w))) \qquad (18)$$

and e is zero at each point of $\mathcal{M}_0$ gives

$$0 = \mathbf{h}(\pi(w)). \qquad (19)$$

The conditions (18) and (19) hold if and only if there exist a triplet of mappings $(\pi(w), \sigma(w), c(w))$ such that

$$\frac{\partial \pi}{\partial w} Sw = \mathbf{f}(\pi(w), c(w), w) \qquad 0 = \mathbf{h}(\pi(w)) \qquad (20)$$

and

$$\frac{\partial \sigma}{\partial w} Sw = \varphi(\sigma(w), \mathbf{k}(\pi(w))) \qquad c(w) = \vartheta(\sigma(w), \mathbf{k}(\pi(w))). \qquad (21)$$

We make use of the following proposition [1, Sec. 1.7].

Proposition 1: Suppose a controller of the form (17) is such that conditions (20) and (21) hold, for some triplet of mappings $(\pi(w), \sigma(w), c(w))$. Suppose that all trajectories of the forced closed-loop system, with initial conditions in a set $\mathcal{X} \times \mathcal{E} \times \mathcal{W}$, are bounded and attracted by the manifold $\mathcal{M}_0$. Then, the controller solves the generalized tracking problem.

The control system (17) in this application is proposed to have the following form:

$$\dot{\xi} = F\xi + Gy \qquad u = H\xi + Ky + \Theta(y). \qquad (22)$$

The controller which satisfies the generalized tracking problem should satisfy (20) and (21). From (20) and (5), $\mathbf{f}^2$ satisfies

$$\mathbf{f}^2(\pi^2, w) = \frac{\partial \pi^2}{\partial w} Sw = \frac{\partial \pi^2}{\partial t} \frac{\partial t}{\partial w} Sw = \frac{\partial \pi^2}{\partial t} \qquad (23)$$

where $x^i = \pi^i(w)$ for $i = 1, 2$. With abuse of notation, we write π instead of $\pi(w)$. Whereas, $\mathbf{f}^1$ satisfies

$$\dot{\pi}^1 = \mathbf{f}^1(\pi^1, c(w), w) = c(w). \qquad (24)$$

Let π^2_{ij} be the ijth entry of the matrix π^2. The second equality of (20) gives the nonlinear control law

$$\tan(\pi^1_1) = \frac{\pi^2_{21}}{\pi^2_{11}} \qquad \tan(\pi^1_2)\sin(\pi^1_1) = \frac{\pi^2_{21}\pi^2_{31}}{(\pi^2_{21})^2 - (\pi^2_{11})^2}. \qquad (25)$$

Equation (21) with the aid of (24) is reformulated to

$$\dot{\pi}^1 = H\sigma + \pi^1 + \Theta(\pi) \qquad \dot{\sigma} = F\sigma + G\pi^1. \qquad (26)$$

Defining $\Theta(\pi)$ as

$$\Theta_1(\pi) = -\tan^{-1}\left(\frac{\pi^2_{21}}{\pi^2_{11}}\right)$$
$$\Theta_2(\pi) = -\tan^{-1}\left(\frac{\pi^2_{21}\pi^2_{31}}{((\pi^2_{21})^2 - (\pi^2_{11})^2)\sin(\pi^1_1)}\right). \qquad (27)$$

Equation (26) is reduced to

$$\dot{\pi}^1 = H\sigma \qquad \dot{\sigma} = F\sigma + G\pi^1 \qquad (28)$$

and the stability of σ and π^1 is guaranteed by having all real parts of the eigenvalues of

$$\begin{bmatrix} H & 0 \\ F & G \end{bmatrix}$$

negative.

VI. RESULTS

A. Real-Time Implementation

The FDI filter was designed by following the described procedure and implemented on the antenna. The Δ block (nonlinearity) is computed using online angular velocity measurements from three gyros at the base of the antenna. The output of the gyros is the vector ω^b_{eb} which by integration and known initial conditions gives the rotation matrix and thus it is possible to compute the error output $\mathbf{h}(x)$ (see [15]).

In order to evaluate the method in a real test scenario, the antenna was mounted on a *ship simulator*. The ship simulator, as shown in Fig. 9, can reliably simulate the movements of the ship in different operational conditions as specified by [18]. It moves the antenna in pitch, roll, and turn axes (It is able to simulate the rotational motions corresponding to 1-2-3 (pitch-roll-turn) Euler angles in [16, Sec. 12.1]). In an antenna laboratory a signal transmitter emulates a virtual satellite and sends signal to the antenna. The lab walls are electromagnetically insulated in order to reduce the effect of the reflection of the signals to the antenna, which makes nonrealistic noise for the beam sensor. In the verification tests, the maximum amplitude and frequency of the pitch, roll, and turn disturbances, according to [18], has been generated by the ship simulator.

B. Design Considerations

The ability to design an FDI system such that the fault estimation is distinguished from the disturbance is highly dependent on the differences in the nature (e.g., frequency) of fault and disturbance. The filter W_f (W_d) has to pass the frequencies which correspond to the fault (disturbance) frequencies in the physical system. Those frequencies are not determined precisely. Here, we provide a comparison on the fault estimation results based on different frequency bands for W_f and W_d. The filters are chosen as band-pass and low-pass Butter Worth filters with cutoff frequencies described in Table I. The results are in conformance with the fault shown in Fig. 5. For brevity reason, only the fault $\hat{\delta}_{f_1} = \left\|\hat{f}_1\right\| sign(\bar{f}_1)/\gamma$ is illustrated in this brief. (The norm is implemented on 0.5 s moving window and the *sign*
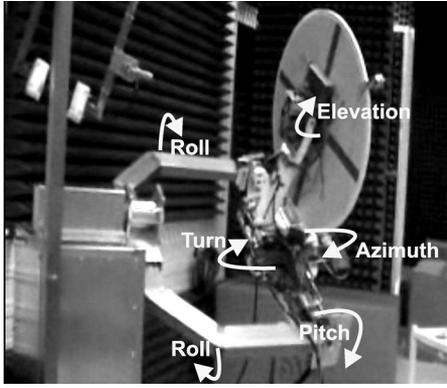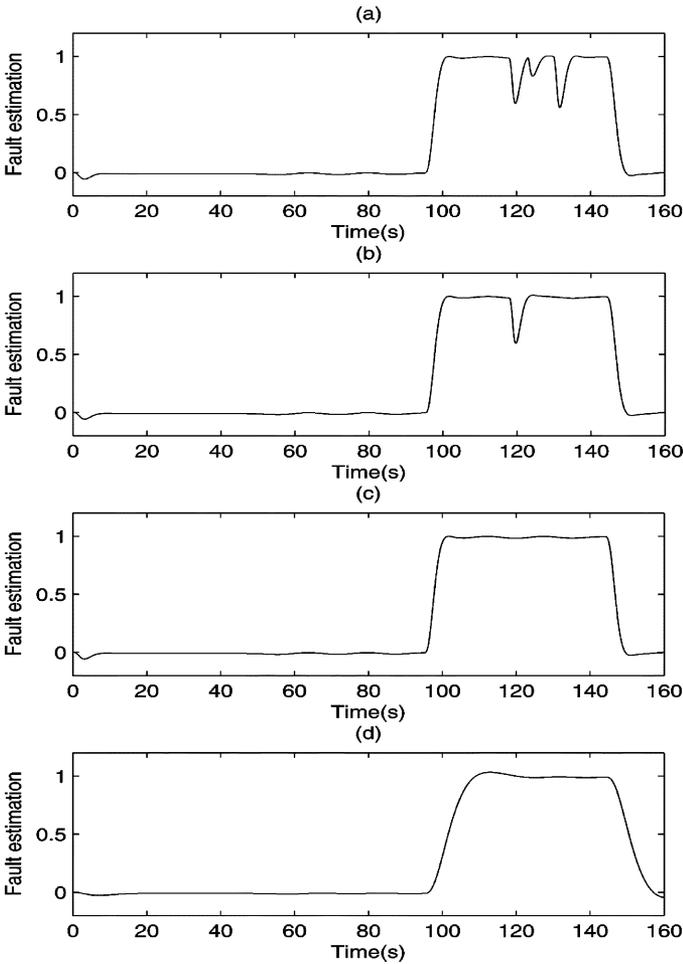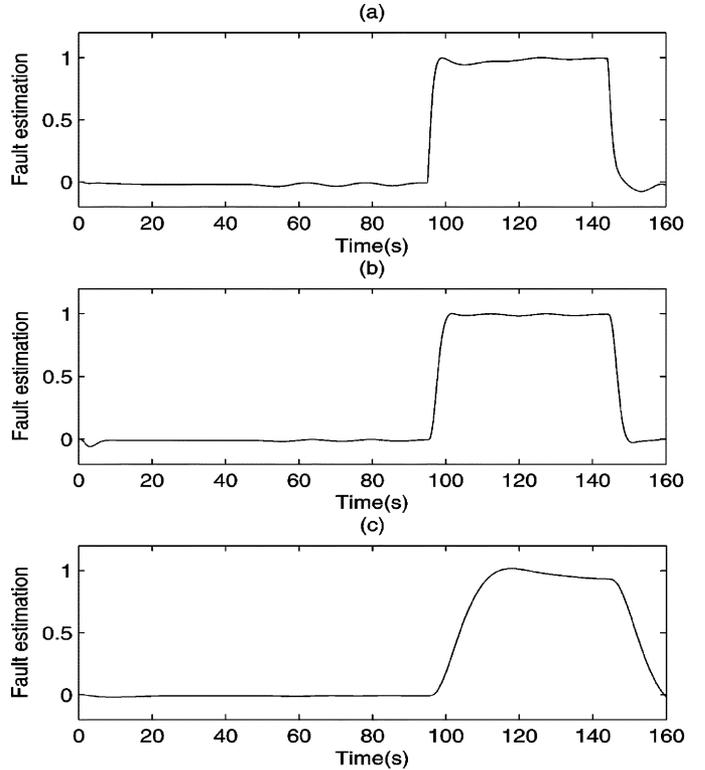
Fig. 9. Illustration of the ship simulator with its rotational axis.

Filter	Type	$\omega_{b_1}(\frac{rad}{s})$	$\omega_{b_2}(\frac{rad}{s})$
W_{f_1}	BW band-pass	1100	1300
W_{f_2}	BW band-pass	600	1300
W_{f_3}	BW band-pass	300	1300
W_{f_4}	BW band-pass	60	1300
W_{d_1}	BW low-pass	-	10
W_{d_2}	BW low-pass	-	1
W_{d_3}	BW low-pass	-	0.1

Fig. 10. Estimated δ_{f_1} using: (a) W_{f_1}; (b) W_{f_2}; (c) W_{f_3}; (d) W_{f_4}.

Fig. 11. Estimated δ_{f_1} using: (a) W_{d_3}; (b) W_{d_2}; (c) W_{d_1}.

function is implemented on $\bar{f}_1$ which is the 0.5 s moving average of $\hat{f}_1$.) In Fig. 10, the results of four different FDI filter designs with respect to each W_f filter and W_{d_2} in Table I are illustrated. The estimated fault shows that by choosing a filter with narrower bandwidth we can detect the fault faster; however at the expense of being more sensitive to the disturbance, e.g., W_{f_1} does not completely cover the fault frequency band in Fig. 6(a). Therefore, the estimation becomes imprecise in Fig. 10(a). On the other hand, using W_{f_4}, that covers a wide range of frequencies, results in a slower FDI filter and hence slower detection/es-

timation [see Fig. 10(d)]. There is indeed a tradeoff between the speed of the detection and the robustness when choosing the fault and disturbance filters for the design of the fault estimator. Fig. 10(b) and (c) show the result of the fault estimation by using W_{f_2} and W_{f_3}, respectively.

Fig. 11 compares the results for different disturbance gain filters, where W_{f_3} is used as the fault gain filter. Choosing a wider band filter, here W_{d_1} in Fig. 11(c), leads to a solution that is less sensitive to the disturbance but at the expense of slower estimation. Conversely, a narrow bandwidth filter, such as W_{d_3} in Fig. 11(a) results in a faster detection but the solution is also more sensitive to the disturbance. Fig. 11(b) shows the result when W_{d_2} is used as the disturbance gain filter.

Fig. 12(a) and (b) show the azimuth and elevation angles before and after the reconfiguration system changes the control method. Fig. 13(a) and (b) show the error calculated by NIMC during the test period. In the non-faulty interval NIMC system is not participating in the control loop but it is forced to calculate the error using the measurements while the beam control car-

This article has been accepted for inclusion in a future issue of this journal. Content is final as presented, with the exception of pagination.

8   IEEE TRANSACTIONS ON CONTROL SYSTEMS TECHNOLOGY
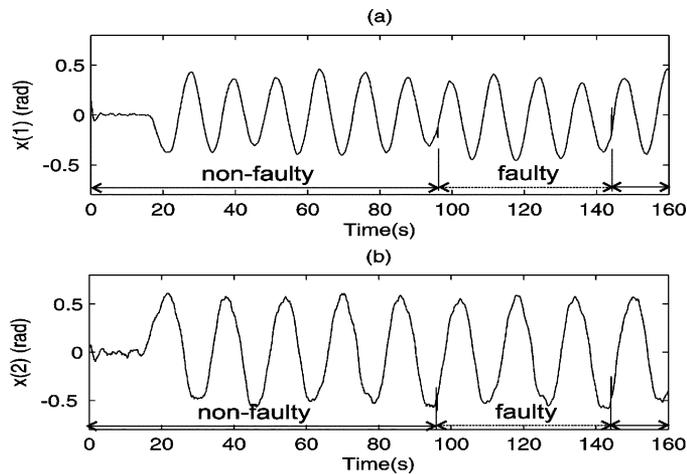
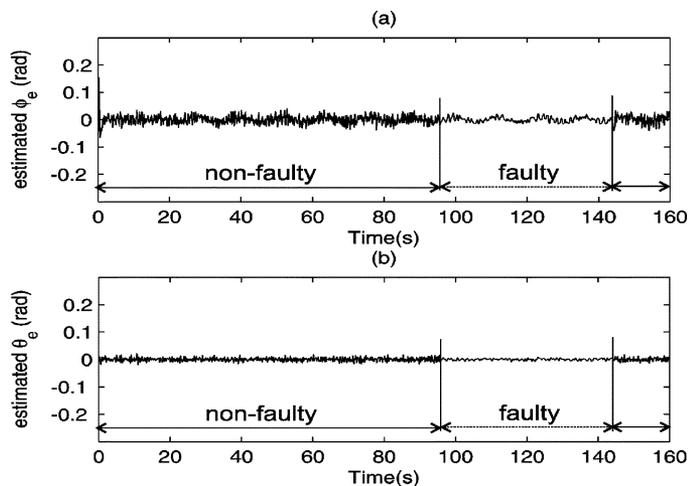Fig. 12.   Motor angles: (a) azimuth and (b) elevation.

Fig. 13.   Calculated errors via IMC (a) elevation and (b) cross-elevation.

ries out the control task. In the faulty interval, NIMC handles the control task.

Finally, it should be noted that the employed fault diagnosis algorithm has been originally proposed for fault estimation purposes. Estimation of the fault in this application has shown to be an extremely challenging task. At present, we restrict ourselves to use the result of the employed method for switching between the controllers. The use of fault estimation in an adaptive reconfiguration system is the subject for further research.

VII. CONCLUSION

The nonlinear dynamical model of the satellite tracking antenna was derived. The model was formulated in a standard problem setup for robust control. A combination of a linear filter—obtained by solving an $\mathcal{H}_\infty$ control problem—and a nonlinear model was employed for the fault detector system. The setup was developed so that the designed FDI system reduces

the effect of the disturbances on the estimated value of the fault. An internal model controller, which guarantees asymptotic convergence of the tracking error to zero, is designed as a secondary control strategy to handle the control task during the faults. Finally, the implemented FTC algorithm has been analyzed on a ship simulator test facility and it has been concluded that the proposed FTC system has fulfilled the desired specifications for STA.

REFERENCES

[1] A. Isidori, L. Marconi, and A. Serrani, *Robust Autonomous Guidance: An Internal Model Approach.*   London, U.K.: Springer, 2003.
[2] A. Isidori, L. Marconi, and A. Serrani, "Robust nonlinear motion control of a helicopter," *IEEE Trans. Autom. Control*, vol. 48, no. 3, pp. 413–426, Mar. 2003.
[3] S. Tanaka and S. Nishifuji, "On-line sensing system of dynamic ship's attitude by use of servo-type accelerometers," *IEEE J. Ocean. Eng.*, vol. 20, pp. 339–346, 1995.
[4] T. Johansen, T. Fossen, S. Sagatun, and F. Nielsen, "Wave synchronizing crane control during water entry in offshore moonpool operation-experimental results," *IEEE J. Ocean. Eng.*, vol. 28, pp. 720–728, 2003.
[5] M. Blanke, M. Kinnaert, J. Lunze, and M. Staroswieski, *Diagnosis and Fault-Tolerant Control.*   New York: Springer, 2006.
[6] R. Isermann, *Fault-Diagnosis Systems: An Introduction from Fault Detection to Fault Tolerance.*   New York: Springer, 2006.
[7] C. Bonivento, A. Isidori, L. Marconi, and A. Paoli, "Implicit fault-tolerant control: application to induction motors," *Automatica*, vol. 40, no. 3, pp. 355–371, 2004.
[8] C. D. Persis and A. Isidori, "A geometric approach to nonlinear fault detection and isolation," *IEEE Trans. Autom. Control*, vol. 46, no. 6, pp. 853–865, Jun. 2001.
[9] C. D. Persis, R. D. Santis, and A. Isidori, "Nonlinear actuator fault detection and isolation for a vtol aircraft," in *Proc. ACC*, 2001, vol. 6, pp. 4449–4454.
[10] R. J. Patton, D. Putra, and S. Klinkhieo, "Friction compensation as a fault tolerant control problem," in *Proc. 23rd IAR Workshop Adv. Control Diagnosis*, U.K., 2008, pp. 20–29.
[11] H. Hammouri, P. Kabore, P. Othman, and J. Biston, "Failour diagnosis and nonlinear observer. Application to a hydraulic process," *J. Franklin Inst.*, vol. 339, no. 4, pp. 455–478, 2002.
[12] R. Kabore and H. Wang, "Design of fault diagnosis filters and faullt-tolerant control for a class of nonlinear systems," *IEEE Trans. Autom. Control*, vol. 46, no. 11, pp. 1805–1810, Nov. 2001.
[13] J. Stoustrup and H. Niemann, "Fault detection and isolation in systems with parametric faults," in *Proc. IFAC*, Beijing, China, 1999, pp. 139–144.
[14] J. Stoustrup and H. Niemann, "Fault estimation-a standard problem approach," *Int. J. Robust Nonlinear Control*, vol. 12, pp. 649–673, 2002.
[15] S. M. N. Soltani, "Model verification of a satellite tracking antenna," Aalborg Univ., Aalborg, 2006.
[16] J. Wertz, *Spacecraft Attitude Determination and Control.*   Norwell, MA: Kluwer, 1978.
[17] T. Fossen, *Marine Control Systems: Guidance, Navigation and Control of Ships, Rigs, and Underwater Vehicles.*   Trondheim, Norway: Marine Cybernetics, 2002.
[18] Inmarsat Global Ltd., London, U.K., "Inmarsat confidential," 2003. [Online]. Available: http://www.alphatelecom.ru/inmarsat/engindex.htm
[19] K. Zhou, J. Doyle, and K. Glover, *Robust and Optimal Control.*   Englewood Cliffs, NJ: Prentice-Hall, 1995.
[20] S. M. N. Soltani, R. Izadi-Zamanabadi, and J. Stoustrup, "Parametric fault estimation based on $\mathcal{H}_\infty$ optimization in a satellite launch vehicle," presented at the IEEE Multi-Conf. Syst. Control (CCA), San Antonio, TX, 2008.
[21] S. M. N. Soltani, R. Izadi-Zamanabadi, and R. Wisniewski, "Robust FDI for a ship-mounted satellite tracking antenna: A nonlinear approach," presented at the IEEE Multi-Conf. Syst. Control (CCA), San Antonio, TX, 2008.